EEET ECOLOGICAL ENGINEERING & ENVIRONMENTAL TECHNOLOGY

Ecological Engineering & Environmental Technology 2022, 23(6), 161–172
https://doi.org/10.12912/27197050/152953
ISSN 2719-7050, License CC-BY 4.0

Received: 2022.08.01
Accepted: 2022.08.24
Published: 2022.09.07

Coupling of Space Remote Sensing and GIS for Detection of Areas at Risk of Degradation (Sidi Mohammed Ben Abdellah Dam Case – Morocco)

Ouakil Abdelhadi[1*], Benhichou Badr[2], Elbelrhiti Kaoutar[1], Amimi Taha[1], Chao Jamal[1], Elbelrhiti Hicham[3]

[1] Laboratory of Natural Resources and Sustainable Development, Faculty of Sciences of Kenitra, University Ibn Tofail, Av. de L'Université, Kénitra, Morocco

[2] Geo-Biodiversity and Natural Patrimony Laboratory, Scientific Institute, Mohammed V University in Rabat, Rabat, Morocco

[3] Department of Fundamental and Applied Sciences (DSFA), Agronomic and Veterinary Institute Hassan II, BP 6202 Madinat ALirfan, Rabat, Morooco

* Corresponding author's e-mail: ouakil.net@gmail.com

ABSTRACT

Sidi Mohamed Ben Abdellah dam watershed is one of the most vulnerable areas of the risk of soil degradation due to its wide exposure, lithological heterogeneity and varying climatic factors. In this sense, the qualitative study of the spatial-temporal evaluation of ground-level occupancy from satellite visualisation data (acquired by the Landsat TM 5 and Landsat TM 8) device derives a land-use map that shows the areas at risk of degradation after the integration of a combination of multiple factors into a GIS geographic information system (climate, terrain, pedology, vegetation cover and human intervention (anti-erosive practice); The results require adaptive vision to better control the phenomenon, to reduce its severity in areas at high risk of soil degradation.

Keywords: USLE, GIS, erosion, watershed, SMBA, Morocco.

INTRODUCTION

Erosion remains a major element of degradation when the soil cannot absorb the excess water from rains. Excess water trickles to its surface and takes away soil particles by generating gullies and ravines. Human activities can reinforce soil degradation through practices like overgrazing, intensification of agriculture, deforestation, urbanisation, etc. (Mahé et al. 2013; Laouina et al. 2010). These anthropic activities cause disturbances in the environment, which promotes erosion and degradation of the natural environment (Roose et al. 1993). Although the importance of agriculture activities for the Moroccan economy and its important contribution to generating incomes for the rural population, it depends on the intra and interannual variabilities of climatic conditions, which also contributes, among other factors, to soil degradation and the way contributes in an indirect way to decrease the incomes of the rural population. According to FAO (1990), the situation continues to worsen, with 40% of the land affected by water erosion. In Morocco, several natural and anthropic factors act on this soil degradation process: climatic aggressiveness and rainfall irregularity, mountainous topography (steep-slope), fragile geological substrates, the succession of drought years (Debbarh, 1997). It is also true that human activities aggravate the fragility of the soil to degradation by anthropic activities like the destruction of plant cover by overgrazing and urbanisation, etc.

Studying the intense variation in climatic factors, determining the prospective detection of degraded areas as well as monitoring, mapping the

evolution and quantification of the erosive phenomenon at the scale of watersheds and sub-watersheds could be a great assist to understand this phenomenon (Roose et al. 1993). For that, it requires the integration of the data set of all prospective elements that could aggravate or limit the spread of this phenomenon in one dataset (Ex. climate and soils). This may allow modelling such phenomena and determining the areas at risk, which allows policymakers to have valuable data to act in areas at risk. Sidi Mohamed Ben Abdellah Sub-watershed (SMBA), located in the western part of northern Morocco (Beaudet, 1969) with an altitude of 1627 at the summit of Jebel Mtourzgane considered the highest point of the study area. It is limited to its North by the Sebou catchment, and by the Wadi Oum-Rbia catchment to its South, it opens to the West of the Atlantic Ocean (Figure 1). The SMBA watershed remains among the important hydrological networks of Morocco, with a surface area

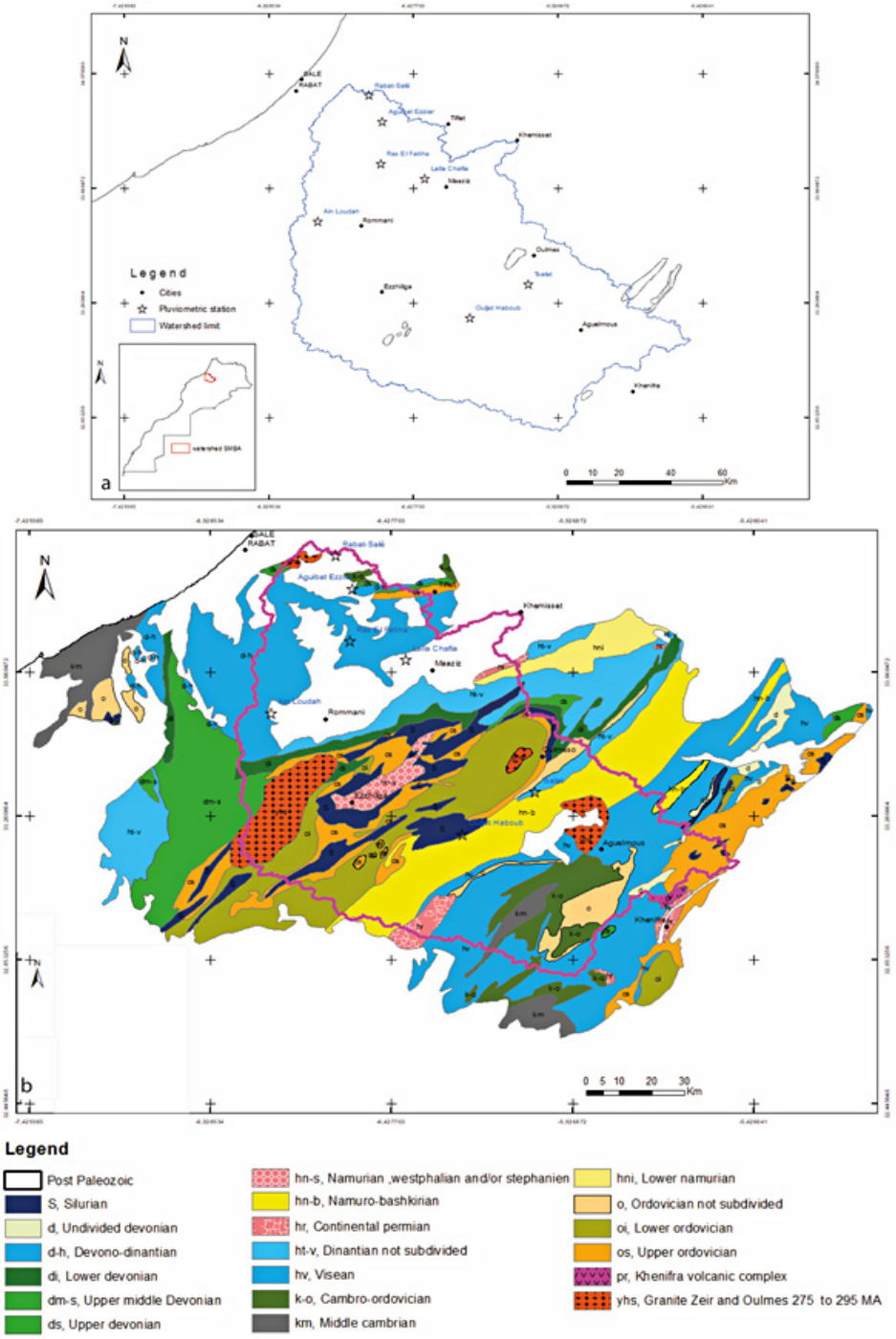

Figure 1. Geographique and geologique situation

of about 10,000 km², it constitutes an environment very exposed to the risk of soil degradation (Mahe et al. 2011). This phenomenon is favoured in particular by the climate changes recorded during these last decades (Khomsi et al. 2014), the pressure of demographic development especially urbanisation and deforestation.

The SMBA Dam is considered, since its construction in 1974, the main reservoir of fresh water that feeds the supply of drinking water to the regions of Rabat-Salé and Casablanca. The reservoir is threatened by several dangers both anthropogenic and natural. Among these dangers appears soil degradation, which favours the silting up of the dam and consequently limits its storage capacity. Hence, the need to understand the erosive phenomenon to limit its propagation is a hot topic. Let's remind that in this theme, a set of models has been developed by researchers. Some models are based on empirical formulae such as the USEL (Universal Soil Loss Equation) of (Wischmeier and Smith, 1978). Others are based on physically parameters measured in the field such as WEPP (Water Erosion Prediction Project) (Fores and Lanc, 1987). Other models are considered hybrid models (also known as semi-empirical) where we combine both empirical and physical measurements collected from the field such as SWAT (Soil and Water Assessment Tools) (Arnold et al. 1996).

The USLE remains the widely used mathematical model for predicting losses due to surface erosion (Wischmeier and Smith, 1978). Based on ancillary data of some factors responsible for the erosive phenomenon as soil type, climate, rainfall, human activities adopted and anti-erosive practices. It allows quantifying the average annual erosion rate for a long period dataset and to plot results to build maps of erosion risks within the studied areas. In this context, Roose and collaborators (2012) indicate that to achieve this ultimate goal of mapping areas at risk of degradation and other goals as to detect degraded areas, to monitor and quantify the evolution of erosion we need to incorporate a set of data directly or indirectly related to the propagation of erosion phenomenon. This can allow a better understanding of the erosive phenomenon at the scale of the whole catchment.

The model developed by Wischmeier and Smith in 1978 allows to estimate the soil particles at risk of erosion and provides a spatialised detection of the surfaces most sensitive to sheet erosion. The universal soil loss equation USLE represents one of the most suitable models for the annual estimation of potential soil water erosion. Indeed, the USLE has been implemented in many northern countries as well as in Morocco (Mati et al. 2000; Boggs et al. 2001; Elbouqdaoui et al. 2005; Dumas et al. 2010).

The objective of this study is the application of the USEL model for a period of 29 years (1985–2014) based on a different data package that represents all factors causing the phenomenon. The land use map generated from a satellite image mosaic (Landsat 8) covering the entire study area; Rainfall station records; the soil map; the slope map restored from the Digital Elevation Model), to be able to identify the areas at risk of degradation.

STUDY AREA

The studied region is the Sidi Mohamed Ben Abdellah sub-catchment, which covers an area of about 2.19% of the total area of the country. It is located in the northwestern part of Morocco (Figure 1). As we mentioned before, the SMBA sub-basin region of study is bounded to the north by the Sebou catchment area and the Oum-Rbia wadi catchment area to the south and opens to the west of the Atlantic Ocean

Several studies have been carried out in the area encompassing the SMBA basin. Researchers are interested in geomorphology (Ex. Beaudet, 1986), soils (Ex. Ghanem et al. 1981.), siltation of dams (Ex. Lahlou, 1986), and geological sediment (Ex. Benmohammadi, 1991). Herein we show the results of some research carried out in the studied region concerning geology, soils and climate. We present also some results that we obtained from the calculation of some climatic indices using a climatic dataset measured directly in the field by different national bodies. This part allows better understanding and better interpretation of the results obtained in the part results and discussions.

Geologyof SMBA watershed

The Bouregreg catchment area as a whole belongs to the Moroccan Massif Central, which occupies 90% of its area. It is the northernmost and most important subsoil bulge of the Hercynian subsoil of Atlantic Morocco. From upstream to downstream of the catchment, we distinguish (Figure 1):

- Kasba Tadla-Azrou Anticlinorium – it constitutes the upper part of the Bouregreg catchment area. It is a veritable mosaic of faulted

anticlines of unequal size where rocks from the Precambrian to the Devonian period emerge and between which are spread the discordant and synclinal depressions of the Carboniferous (Termier, 1936; Bouabdelli, 1989). The continental foundations of the Khenifra's Permian cover the central-eastern part of this complex in angular discordance.

- Fourhal Synclinorium – it is a Syncline gutter from the north of Boujad to the Causse d'Agourai that, exposes the sandstones and shales of Namur and Westphalia to erosion (Tahiri, 1991). Its eastern flank is pierced by the granitic intrusion Ment.
- Khouribga-Oulmès Anticlinorium – forms the centre of the Bouregreg watershed. Facing NE-SW, it carries in height the mainly schistose and quartzitic layers of the Ordovician and Silurian, on which are placed some detritus and/or carbonate scarves of the Carboniferous (Piqué, 1979; Chakiri, 1991; Tahiri, 1991). Several granitoid massifs were built there, including Zaër, Oulmès and Moulay Bou Azza.
- The synclinorium of Khémisset-Rommani – it is a thick synclinal mass essentially constituted by schisto-sandstone layers of the Lower Carboniferous (Tournaisian and Viséen) and Triassic argillites and basalt. The whole is sometimes eroded as it passes through anticlines where Devonian formations emerge (Chakiri, 1991; Zahraoui, 1991).
- Rabat-Tiflet Anticlinorium – it is a remarkable East-West oriented structure, where cataclastic granite and New Caledonian metamorphic rocks emerge as a result of accidents (Piqué, 1979; El Hassani, 1990).

Climate in the SMBA watershed

According to (Bensalah 2008), the climate in the catchment area is influenced both by the altitude, especially in the north where it can reach 1,630 m, and by the opening to the Atlantic Ocean, which provides humidification and temperature moderation. We collect data on some climatic parameters of the SMBA catchment. Table 1 shows the monthly average of annual precipitation for the period from 1980 to 2009 in several cities and villages in the studied region. We can clearly deduce that the year can be subdivided into two seasons. A rainy season from October to May and a dry season from June to September. In addition, the maximum precipitation is observed during December while the Minimum is in July.

Another way to analyse this climatic data is to measure different climatic indexes, especially those widely used in Morocco and North Africa. In this context, we are first interested in De Martonne's aridity index calculated using the formulae:

$$I = P/(T+10) \quad (1)$$

where: P – the total annual precipitation; T – the average annual temperature.

The results presented in Figure 2 show that the catchment is characterised by a Semi-Arid climate with a minimum value of 10 and a maximum value of 18.25 in the Rabat Salé regions. We also calculate De Martonne's monthly aridity index given by the equation:

$$I = 12P/(T+10) \quad (2)$$

Here again, the results show that we have two major contrasting seasons. An arid season from July to August with a maximum severity is July

Table 1. Average monthly annual precipitation for the period 1980–2009 (SIGMED, 2014)

Station	Sep	Oct	Nov	Dec	Jan	Feb	Mar	Apr	May	June	July	Aug	Annuel Sum
Sidi Jabbour	12.4	29.0	45.2	48.1	45.4	41.9	36.5	30.3	17.5	6.9	0.9	0.8	314.9
Aguibat Ezziar	9.5	34.8	68.7	76.1	67.8	56.6	46.6	42.7	22.4	6.9	0.5	0.9	433.5
Ras EL Fatiha	10.3	31.1	60.5	69.9	59.1	53.0	45.3	37.4	16.1	5.3	0.8	1.4	390.2
Lalla Chafia	12.1	30.4	49.2	52.8	51.0	45.4	40.9	40.1	17.6	5.2	0.3	0.6	345.6
Ouljet Haboub	11.9	22.0	33.3	40.5	30.6	37.6	33.6	28.4	17.6	9.5	3.5	3.9	272.4
Ain Loudah	11.0	28.7	54.3	56.9	54.3	50.1	38.0	33.2	16.6	3.9	0.9	1.2	349.1
Tsalat	16.3	34.8	62.7	77.9	67.5	64.7	55.6	42.6	27.9	11.1	5.6	4.6	471.3
Rabat-Salé	8.6	42.8	67.3	104.8	79.0	61.3	52.0	55.2	20.4	4.0	0.2	1.2	496.8
Max	16.3	42.8	68.7	104.8	79.0	64.7	55.6	55.2	27.9	11.1	5.6	4.6	496.8
Min	8.6	22.0	33.3	40.5	30.6	37.6	33.6	28.4	16.1	3.9	0.2	0.6	272.4
Average monthly	11.5	31.7	55.2	65.9	56.8	51.3	43.6	38.7	19.5	6.6	1.6	1.8	384.2

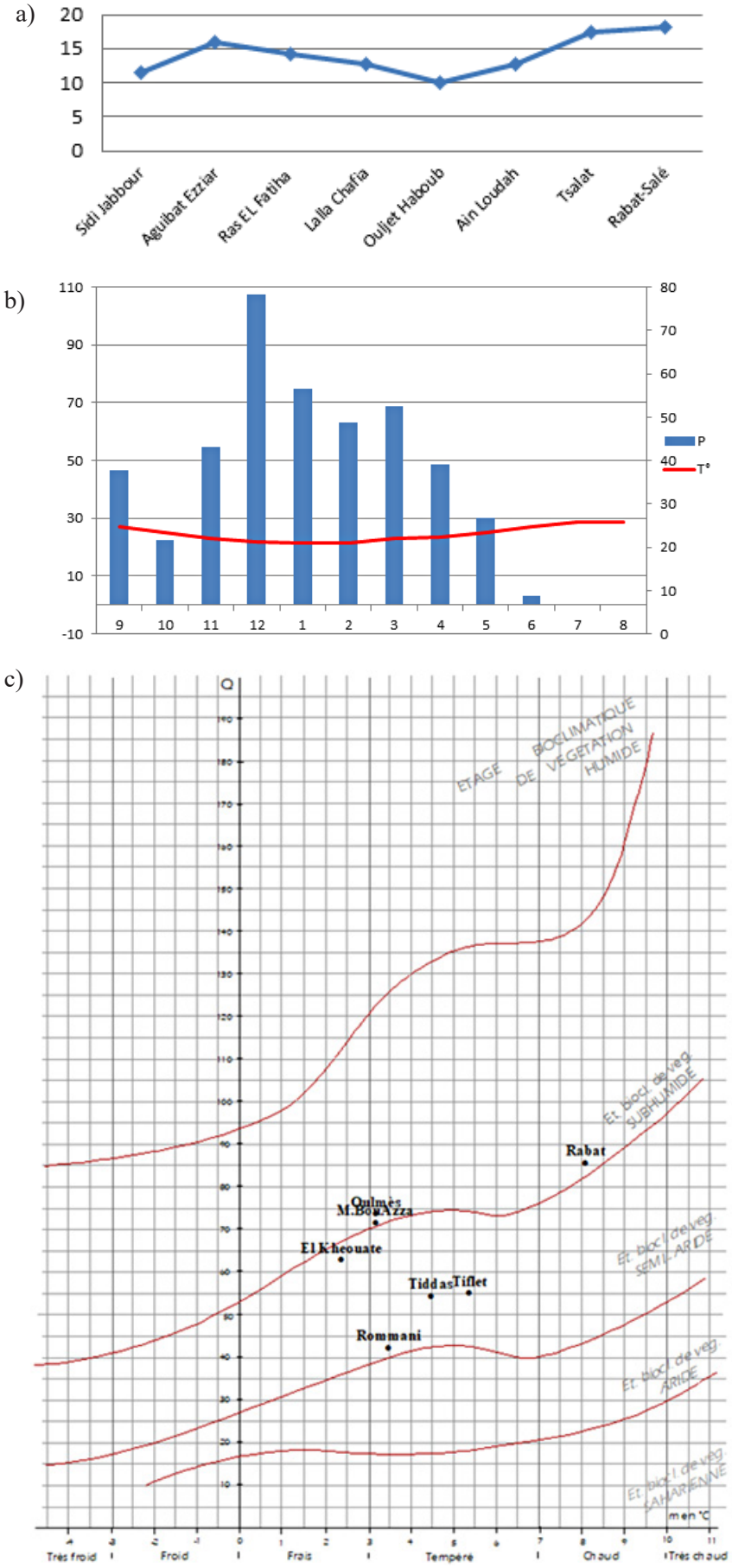

Figure 2. a) Variation of the Marton index; b) Diagramme ombrothermique; c) Emberger rainfall quotient

when the temperature records 24.5°C. The other season considered the least arid period starts in December and goes until February. It is characterised by monthly De Martonne indices between 34.82 and 39.13. This particularity is related to the heavy rains that mark this time of year. However, contrary to the first lecture of the amount of precipitation that allows characterising only two contrasting seasons, the study of the monthly De Martonne indice shows that the month of September, with an index of 2.86, is considered an arid month with a semi-arid tendency since rainfall is more abundant than in June, July and August.

This question of dry and humid seasons during the year is crucial and directly influences the vegetation cover (Gaussen, 1953) which is considered one of the paramount factors influencing erosion. Figure 2b, shows the ombrothermic diagrams of some stations in the studied region (Bagnouls and Gaussen, 1953). We can see that the humid season runs from October to April when the temperature reaches its maximum values in July and August.

Another climatic parameter that we calculate is the Emberger Rainfall quotient (Quotient pluviométrique d'Emberger) very used in the Mediterranean region (Figure 2c):

$$Q = (2000 \cdot P)/M2–m2 \quad (3)$$

where: P – the average annual precipitation in (mm); M – the average of the hottest month maxima in $K°$; m – the average minimum for the coldest month in $K°$; the values of Q for the available stations are listed in Table 2.

From the study of the climatic parameters using different climatic indices, we can clearly deduce that: the watershed of SMBA extends largely in the semi-arid climatic domain and that just the region of Oulmès is characterised by a sub-humid climate. This has a direct influence on vegetation, which is one of the key parameters that control erosion. In addition, we conclude that the region has two major contrasting seasons, an arid season and another season, considered as least arid period.

MATERIALS AND METHODS

Materials sources and data

For this study, we collected a series of Landsat 7 and Landsat 8 images freely available from Glovis database (https://glovis.usgs.gov) (Table 3). These images cover 29 years. We download a DEM as a courtesy of the same database (http://glovis.usgs.gov). The DEM used has a resolution of 30 m. We also digitalised different geologic formations and lithology from the geological map of Morocco at 1 / 1,000,000. Concerning soils, we used different soil maps. The most important is the soil map of Bouregreg (Ghanem et al. 1981). To cover the totality of the studied area, we also used partially other soil maps such as the soil map of the Chaouia N.E. and Sehouls Zaers (Maheet al. 2013**)** and the soil map of the Bouregreg catchment (Zamblé, 2014) (Figure 3).

Methods

The assessment and the control of erosion risks require the analysis and integration of the different factors that promote erosive processes (terrain topography, soil erodibility, and land use). Our approach is based on the use of spatial remote sensing data to produce land use land cover (LULC) maps for different periods. To reach this goal, and using ARCG GIS 10.2 and ERDAS imagine 2015, we followed these steps (Figure 4). First, we start with visual interpretation based on our knowledge of the studied area. Then, we applied the unsupervised classification using K-means model and both single-band and multiband supervised classification using regions

Table 2. Emberger rainfall quotient Q

Station	P	M	m	Q	Bioclimatic classification
Tiflet	487.3	35.5	5.4	55.17	Semi-arid climate
Rabat	496.6	28	8.1	85.74	Semi-arid climate
M. BouAzza	600	32	3.2	71.69	Semi-arid climate
Oulmès	658.3	33.8	3.2	73.8	Subhumide climat
Tiddas	478	34.5	4.5	54.47	Semi-aride climat
Rommani	387.2	34.8	3.5	42.34	Semi-arid climate
El Kheouate	543	32.1	2.4	62.99	Semi-arid climate

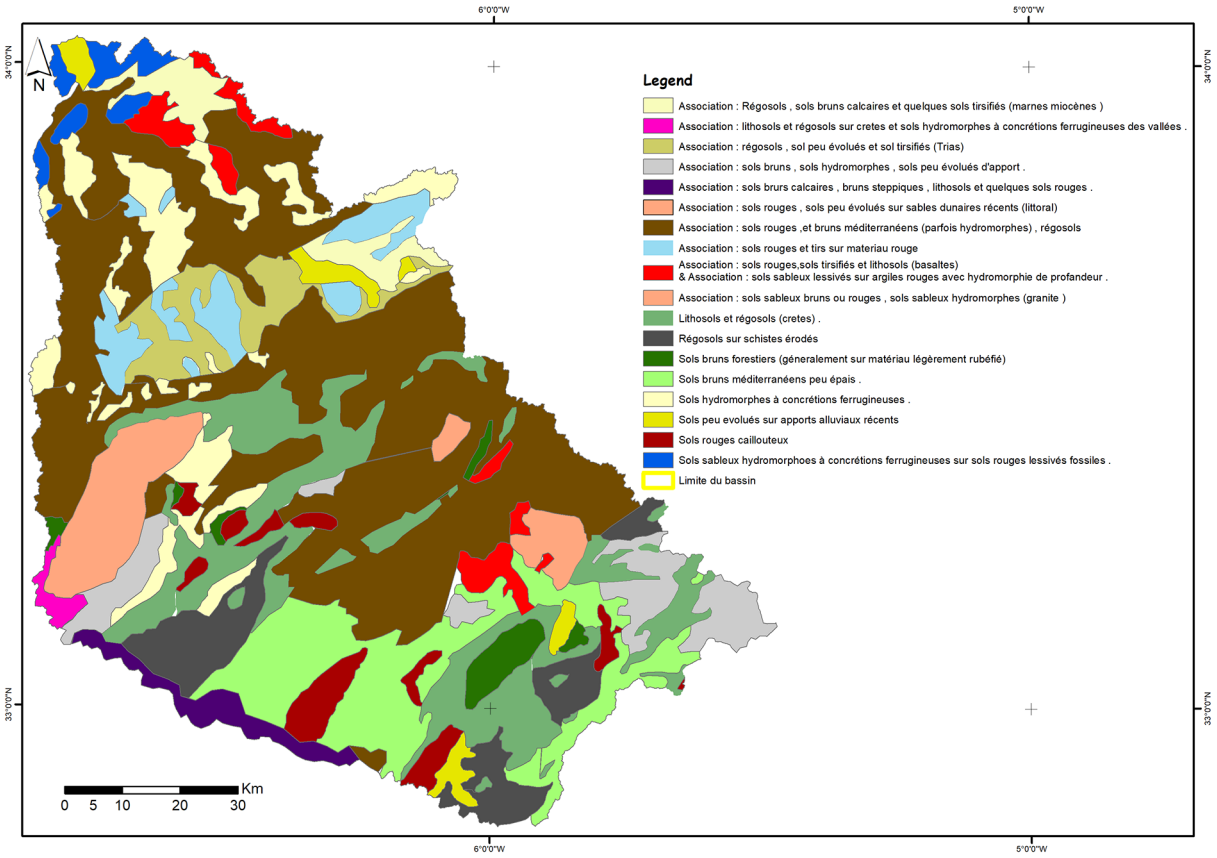

Figure 3. Soil map

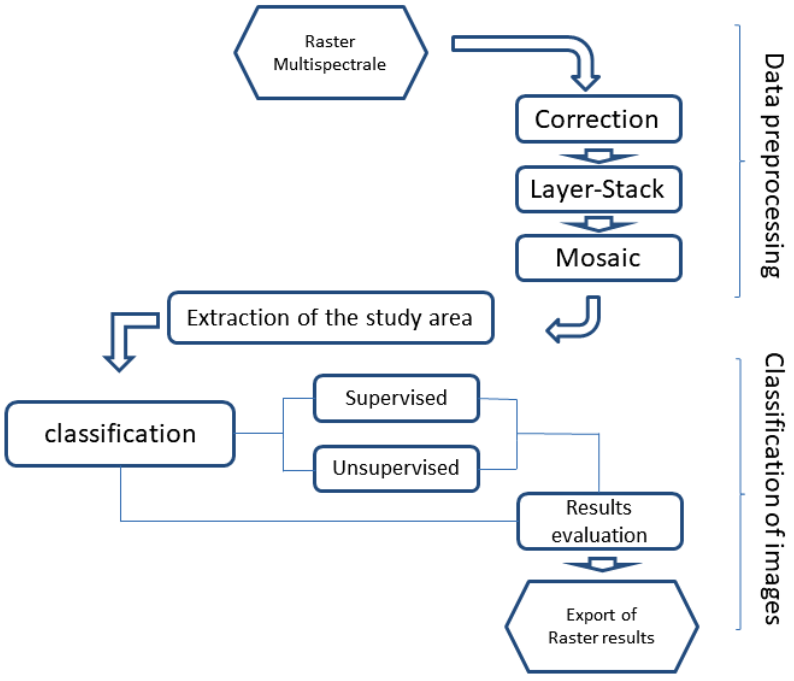

Figure 4. Approach followed for land use mapping

of interest and SVM model. Once the classification is completed, and always based on our field knowledge, we start the post-classification process by combining similar results. When the land use maps of different periods are produced, we apply techniques and operations to produce a

map of changes in land use throughout the study area. The most recent map of changes produced was used to produce an erosion sensitivity map through the application of the Wishmeier and Smith on USEL model.

Description of Wishmeier and Smith on USEL model

The Wischmeier and Smith model was calculated using the formula:

$$A = R \times K \times LS \times LS \times C \times P \quad (4)$$

where: A – land loss rate in tonnes per hectare per year (t/ha/year); R – erosivity of rainfall in Megajoules in millimetres per hectare hour (MJ.mm/ha. h); K – Soil erodibility in tonne hours per Megajoule millimetre (t.h/MJ.mm); LS – slope and inclination length (without unit); C – vegetation cover factor (without unit); P – factor taking into account anti-erosion practices (without unit).

R factor estimation

The R-factor measures the kinetic energy of the rain, and it requires measurements of rainfall intensity (Wischmeir and Smith, 1978). To produce the rainfall's erosivity map the rain erosion factor is calculated according to the following equation:

$$\mathrm{Log}R = 1.744 \times \mathrm{Log}\,(P_i^2/P) + 1.299 \quad (5)$$

where: R – rain aggressiveness index in units/years; P – average annual precipitation of the observation time (mm); P_i – average monthly precipitation (mm).

LS factor estimation

LS-factor describes the effects of slope length and slope steepness on soil erosion (Wischmeir and Smith 1978). It is influenced by several factors. Generally, we talk about the intrinsic parameters of the soil like the structural stability, soil texture and the rate of organic matter. Furthermore, the topography is another factor that influences soil erodibility. To integrate the topography in our model, we use the DEM to produce a slop length and inclination map according to Wishmer and Smith (1978):

$$LS = (X/22.1)^m \times \times (0.065 + 0.045 \cdot S + 0.0065 \cdot S^2) \quad (6)$$

where: X – the length of the slope (m); S – the gradient of the slope (%); m – coefficient varies according to the slope.

The values of X and S can be obtained from the digital elevation model (DEM). To calculate the X value, the flow accumulation was derived from the DEM after performing the flow direction and filling processes in the GIS tool.

$$X = \text{the accumulation of the flow rate} \times \text{resolution} \quad (7)$$

By substituting the value X, the equation becomes:

$$LS = [(\text{the accumulation of the flow rate} \times \times \text{resolution})/22.1]^m \times \times (0.065 + 0.045 \cdot S + 0.0065 \cdot S^2) \quad (8)$$

The gradient of the slope (%) was taken from the DEM coupled with a GIS system, and the value of m was obtained from Table 4. It presents variation of the gradient of the slope according to its inclination.

K factor estimation

This factor depends essentially on the physical and chemical properties of the soil (organic matter content, structural stability, porosity). It represents the sensitivity of the soil to be eroded by rain – the deeper the soil, the more resistant it is to the risk of erosion (Ryan, 1982). According to the formula of Wischmeier and Smith (1978) which is based on soil texture M = (% fine sand + % silt) × (100 – % clay), organic matter content (a), soil structure (b) and permeability (c)

C factor estimation

The C factor is interested in the effects of vegetation, management and erosion control practices on soil loss (Wischmeir and Smith, 1978). The

Table 3. List of Landsat images used from Glovis database

SPACECRAFT_ID	DATE_ACQUIRED	WRS_PATH	WRS_ROW	SENSOR_ID	SENSOR_MODE	LANDSAT_SCENE_ID
LANDSAT_7	27/05/2003	201	36	ETM	SAM	LE72010362003147ASN00
LANDSAT_7	27/05/2003	201	37	ETM	SAM	LE72010372003147ASN00
LANDSAT_7	18/05/2003	202	36	ETM	SAM	LE72020362003138MPS02
LANDSAT_7	18/05/2003	202	37	ETM	SAM	LE72020372003138MPS02

Table 4. Variation of the gradient of the slope according to its inclination

m	Slope %
0.5	>5
0.4	3–5
0.3	1–3
0.2	<1

Table 5. Index value C by occupation type

Occupation type	Indice C
1 – Water	0
2 – Building	0.2
3 – Dense vegetation	0.001
4 – Bare soil	1
5 – Varied vegetation	0.5

C-factor's value varies from 1 in completely bare land to 0 in a water body or completely covered land surface (Table 5). It is important to notice the *C* factor varies with time and spatially and for that reason, many studies use remote sensing tools to quantify land cover units, *C* factor and its spatial and temporal variabilities (Kebede et al. 2021). We also based on remote sensing techniques to establish a land-use map. This map represents the distribution of the five classes:

The P factor

The last factor used is the anthropic factor *P*, which represents the contribution of human intervention to reducing the erosive effect in the region through the implementation of anti-erosion approaches. This factor varies between 0 for a fully protected area and 1 for an area at risk. In our case, the study area shows a total absence of all types of anti-erosion interventions, for which an average value of 1 is assigned to the entire area.

RESULTS AND DISCUSSIONS

Figure 5 shows the produced land use map. The studied area is divided into 5 classes. The first is the areas occupied by water, which represent 10% where the vegetation covers about 25%. Concerning the areas used by men are divided into agricultural areas occupying 15% and buildings represented by 20%. The last class is the barren soil presented by 40% of the mapped area.

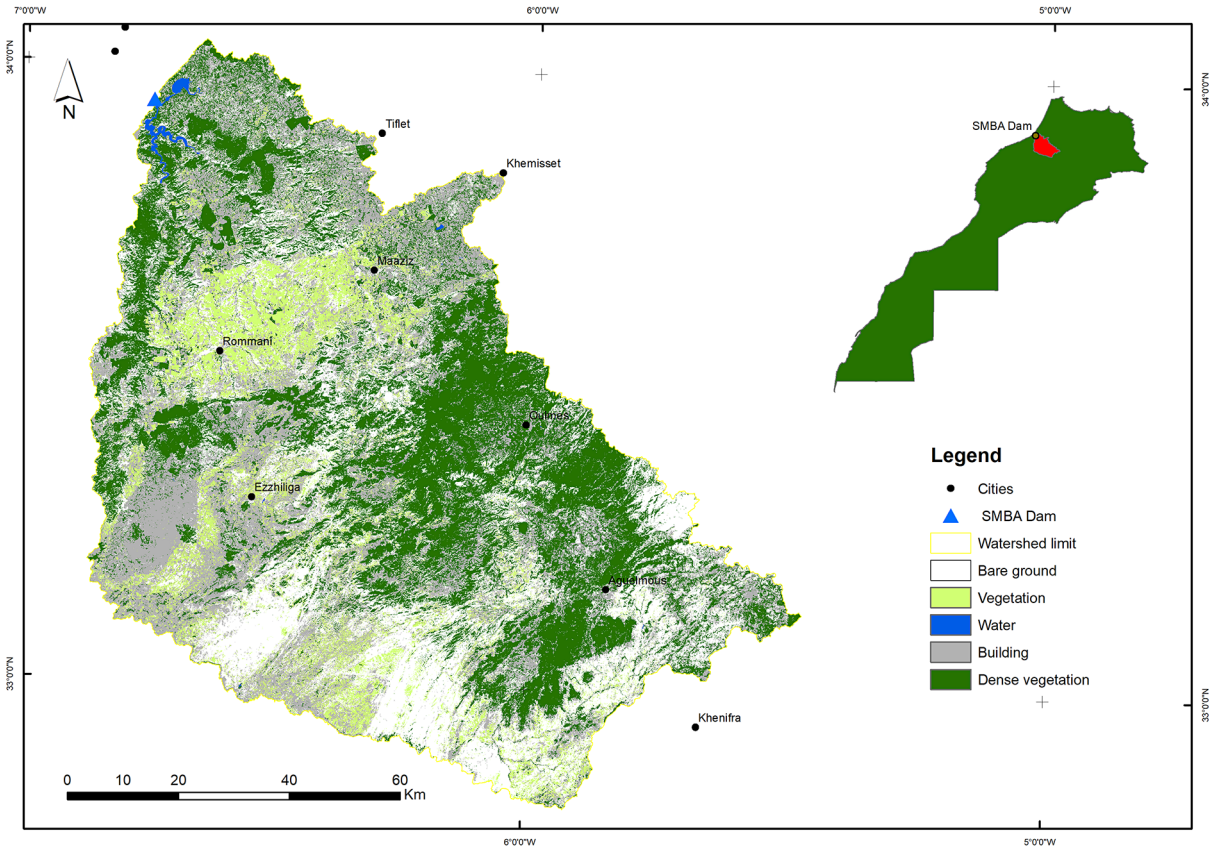

Figure 5. Land use map of the Sidi Mohamed ben Abdellah watershed

From the first results, we can clearly see that the area occupied by vegetation represents 40%, these areas are theoretically protected from erosion; on the other hand, the areas threatened (areas exposed to the risk of degradation) represents 60%. The next factor was the slope, which is presented in the map shown in Figure 6. In this figure, we can clearly see that the majority of the land represents high values of the *LS* factor (topographic factor). According to a study conducted by Roose (2001) there is a relationship between slope gradient and rates of erosion on agricultural land. In fact, scientists have shown that topography affects runoff and soil losses through two components: the degree of slope and the length of the steepest slope (Wischmeier and Smith, 1978). In this way, the greater degree of slope inclination is responsible for the greater kinetic energy of the flow and the detachability of particles from the ground (Hadir, 2010). Similarly, the longest slopes allow a higher accumulation of runoff, which increases the overall energy of the slope and its detachment and transport possibilities (Batti, 2007).

The erosion sensitivity map is produced in Figure 7. It shows the detection of areas at risk of degradation the percentage of the surface area exposed and highly exposed to the risk of erosion, which is clearly presented by the previous factors acting on this phenomenon. Agricultural areas, limited to arid and semi-arid zones, lead to excessive exploitation of the soil which develops the risk of degradation.

CONCLUSIONS

This study shows that the use of updated cartography of the land use map derived from satellite images coupled with data characterising better the environment (Pedology, Climate, Geology) helps to detect areas highly exposed to the risk of degradation.

The SMBA dam watershed has been marked by a very significant variation in land use, all due to the variation in rainfall patterns, unfavourable climatic conditions that have caused the degradation of the vegetation cover and consequently the exposure of the soil to the risk of erosion, as well as the intense migration of the population to cities and non-directed land use has increased the degree of soil sensitivity. Spatial remote sensing and geographic information systems serve as tools for monitoring land cover change to better understand erosion in order to apply and monitor adaptive strategies.

The results show that the percentage of degraded land is continuously increasing, not only due to the disruption of the climate regime (usually temperature and precipitation), but also to the undirected use of land as a result of intense population demographic change, and migration to urban areas. Any adaptation strategy requires a set of multidisciplinary rules to better control the phenomenon.

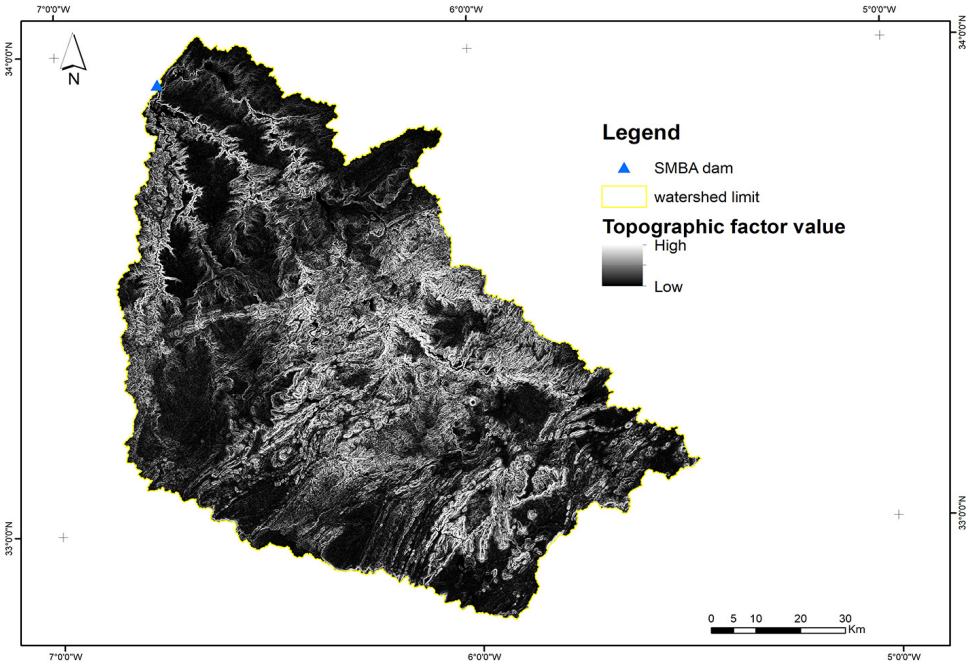

Figure 6. Map of the topographic factor of the Sidi Mohamed ben Abdellah watershed

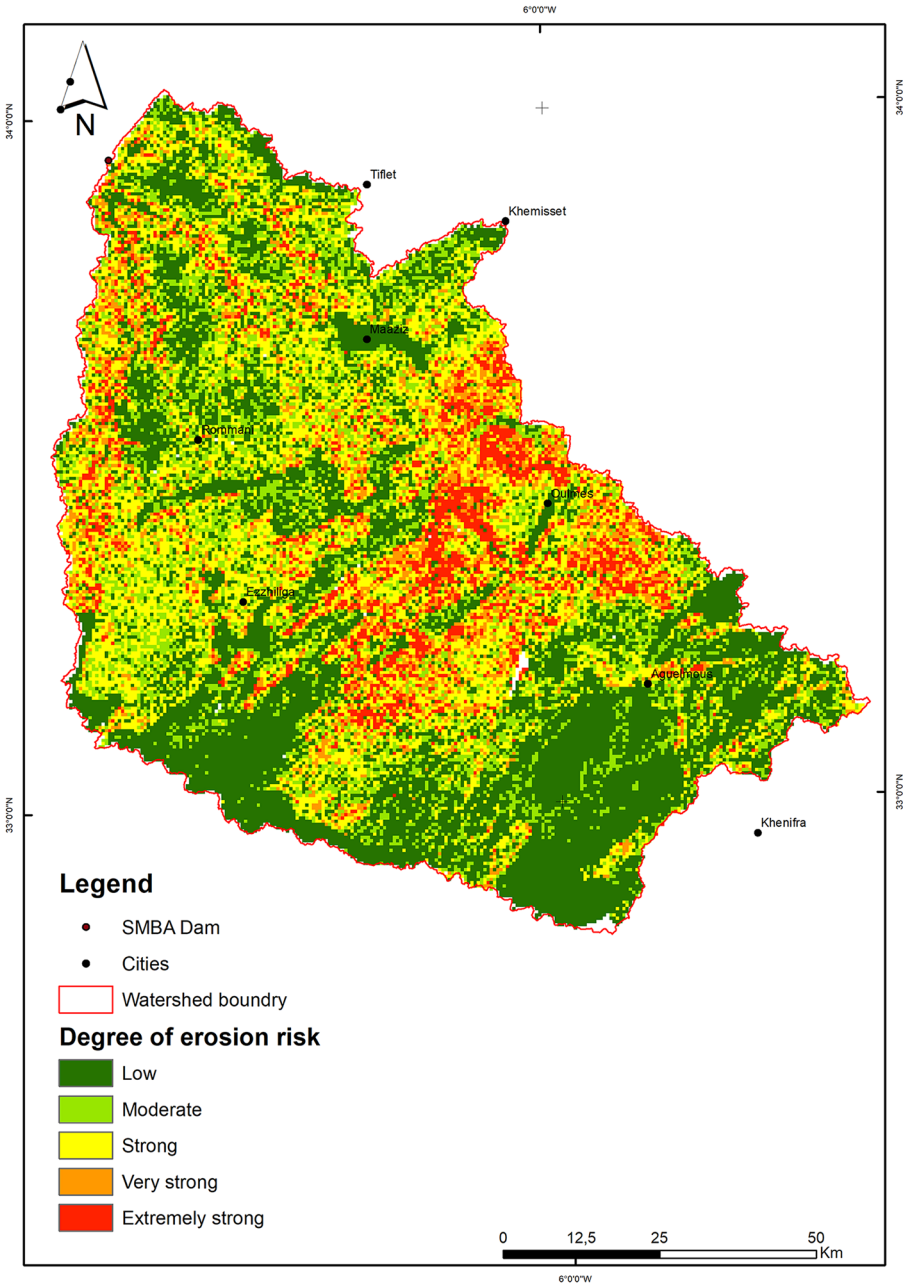

Figure 7. Map of sensitivity to average erosion at the level of the Sidi Mohamed ben Abdellah watershed

REFERENCES

1. Arnold J.G., Srinivasan R., Muttiah R.S., Williams J.R. 1998. Large-area hydrologic modelling and assessment: Part I Medel development. Journal of American Water Resources Association.
2. Bagnouls et Gaussen. 1953. Saison sèche et indice xérothermique. Bull. Soc. Hist. Nat. de Toulouse, 88, 193–240.
3. Beaudet, G. 1969. Le plateau central marocain et ses bordures: étude géomorphologique. Thèse de Lettres.Imprimerie française, Rabat.
4. Bensalah N. 2008. Indicateurs des risques de ruissellement et d'érosion en vue d'une gestion durable des eaux et des sols (Bassin versant de Bouregreg).Thèse de doctorat de géographie, Université Mohammed V-Agdal, Faculté des Lettres et des Sciences Humaines, Rabat (Maroc).
5. Boggs, G.S., Devonport C.C., Evans K.G., Saynor M.J., Moliere D.R. 2001. Development of a GIS based approach to mining risk assessment. Supervising Scientist Report. Environment Australia, Darwin, 159, 49.
6. Bouabdelli M. 1989. Tectonique et sédimentation dans un bassin orogénique: le sillon viséen D'Azrou-Khénifra (Est du Massif hercynien central du Maroc). Thèse Doctorat es-Sciences, Strasbourg, 259.

7. Chakiri S. 1991. Le Paléozoïque de la région de Tsili-Tiddas (Maroc central occidental),Stratigraphie, Sédimentologie et évolution structurale hercynienne. Thèse de 3ème Cycle, Univ. Rabat, 227.
8. Debbarh A. 1997. Irrigation et développement durable :aspects environnementaux. Options Méditerr., A, 31, Séminaires Méditerranéens, 357–365.
9. Dumas P., Fossey M. 2009. Mapping Potential Soil Erosion in the Pacific Islands. A case study of Efate Island (Vanuatu), Proceedings 11Th Pacific Science Inter Congress, Pacific Countries and their ocean, facing local and global changes, Tahiti French Polynesia.
10. Dumas P., Printemps J. 2010. Assessment of soil erosion using USLE model and GIS for integrated watershed and coastal zone management in the South Pacific Islands. Proc. Interpraevent, International Symposium in Pacific Rim, Taipei, Taiwan, 856–866.
11. Dumas P., Printemps J., Mangeas M., Luneau G. 2010. Developing erosion models for integrated coastal zone management. A Case Study of New-Caledonia West Coast, Marine Pollution Bulletin, 161, 519–529.
12. El Hassani A. 1990. La bordure nord de la chaîne hercynienne du Maroc, chaîne calidonièn ne.
13. Elbouqdaoui K., Ezzine H., Badrahoui M., Rouchdi M., Zahraoui M., Ozer M. 2005. Approche méthodologique par télédétection et SIG de l'évaluation du risque potentiel d'érosion hydrique des sols sur le bassin versant de l'oued Srou (Moyen-Atlas, Maroc). GeoEcoTrop, 29, 25–36.
14. FAO. 1994. Organisation des Nations Unis pour l'Alimentation et l'Agriculture. Introduction à la gestion conservatoire de l'eau, de la biomasse et de la fertilité des sols (CGES). Bulletin Pédologique de la FAO, 70, 420.
15. Kebede Y.S., Endalamaw N.T., Sinshaw G.B., Atinkut B.H. 2021. Modeling soil erosion using RUSLE and GIS at watershed level in the upper beles, Ethiopia. Environmental Challenges, 2, 100009. https://doi.org/10.1016/j.envc.2020.100009
16. Khomsi K., Mahe G., Sinan M., Snoussi M. 2014. Evolution des évènements chauds rares dans les bassins versants de Tensift et Bouregreg. In: Laouina, A. & Mahe, G. (Eds.), Gestion durable des terres. Proceedings de la réunion multi-acteurs sur le bassin du Bouregreg. CERGéo, Faculté des Lettres et Sciences Humaines, Université Mohammed V-Agdal, Rabat 2013. Edité par ARGDT, Rabat, Marocco.
17. Laouina A., Aderghal M., AI Km'kouri 1., Chaker M., Machmachi 1., Machouri N., Sfa M. 2010. Utilisation des sols, ruissellement et dégradation des terres, le cas du secteur Sehoul, région atlantique,-Maroc. Sécheresse, 21(4), 309–316.
18. Mahe G., Aksoy H., Brou Y.T, Meddi M., Roose E. 2013b. Relationships between man, environment and sediment transport: a spatial approach. Revue des Sciences de l'Eau, 26(3), 235–244.
19. Mahe G., Benabdelfadel H., Dieulin C,. Elbaraka M., Ezzaouini M., Khomsi K., Rouche N., Sinan Snoussi M., Trabi M., Zerouali A. 2014. Evolution des débits liquides et solides du Bouregreg. Quantification des MES au Bassin versant du Bouregreg, méthode MUSLE.
20. Mati B.M., Morgan R.P.C., Gichuki F.N., Quinton J.N., Brewer T.R., Liniger H.P. 2000. Assessment of erosion hazard with the USLE and GIS: A case study of the Upper EwasoNg'iro North basin of Kenya. International Journal of Applied Earth Observation and Geoinformation, 2(2), 78–86. DOI: 10.1016/S0303-2434(00)85002-3
21. Piqué A. 1979. Evolution structurale d'un segment de la chaîne hercynienne: la Meseta marocaine Nordoccidentale. Sci. Géol., Mém., Strasbourg, 56, 253.
22. Roose E. 2001. GIS erosion risk assessment of the Piracicaba River Basin, southeastern Brazil, GI-Sciences and Remote Sensing, 38, 157–171.
23. Roose E., Arabi M., Brahamia K., Chebbani R., Mazour M., Morsli B. 1993. Erosion en nappe et ruissellement en montagne méditerranéenne algérienne.Réduction des risques érosifs et intensification sur la production agricole par la GCES:synthèse des campagnes 1984–1995 sur un réseau de 50 parcelles d'érosion. Cahiers ORSTOM, Série Pédologie, 28(2), 289–308.
24. Roose E., Sabir M., Arabi M., Morsli B., Mazour M. Soixante années de recherches en coopération sur l'érosion hydrique et la lutte antiérosive au Maghreb. Physio-Géo, 6(1), 43–69.
25. Ryan J. 1982. A perspective on son erosion and conservation in Lebanon. Publication 69, American University of Beirut, 15–38.
26. Samaali H. 2011. Etude de l'évolution de l'occupation et de l'utilisation du sol dans le delta de Mejerda par télédétection et systèmes d'informations géographiques. Thèse du Doctorat en Géographie, Université de Tunis, Tunis (Tunisie).
27. Tahiri A. 1991. Le Maroc central septentrional: Stratigraphie, Sédimentologie et Tectonique du Paléozoïque; Un exemple de passage des zones internes aux zones externes de la chaîne hercynienne du Maroc. Doctorat ès-Sciences, Univ de Bretagne Occidentale, Brest, France, 300.
28. Termier H. 1936. Etudes géologiques sur le Maroc Central et le Moyen Atlas septentrional. Notes et M. Serv. Des Mines et de la carte géologique, Rabat, 33(3).
29. Wachal D.J., Hudak P.F. 2000. Mapping land slide susceptibility in travis conty, USA, GeoJournal, 51.
30. Wischmeier W.H., Smith D.D. 1978. Predicting rainfall erosion losses. A guide to conservation planning. Édit. US Department of Agriculture, Washington, 537, 58.
31. Zahraoui M. 1991. La plate-forme carbonatée dévonienne du Maroc occidental et sa dislocation hercynienne. Thèse ès Sciences, Univ. Bretagne Occidentale, Brest, 261.